appeared to provide 3D volume-rendering options, they could not identify specific areas such as tumour remnants, which surgeons require to discriminate between the tumour and the surrounding normal tissues [7–9]. Another study focused on a pre-operative diagnosis, although it provided segmentation and a 3D image of the region of interest (ROI) [10]. To our knowledge, the intra-operative computation and visualization of tumour remnants on the basis of the trace log of electrocautery have not been reported thus far.

To improve previous navigation systems, we added a tumour segmentation module and an analyzer to the electrocautery trace log. Since the trace analyzer provides details on the removed volume and residual tumour tissues without additional MR scanning, the surgeon can reduce the number of scans, which would otherwise extend the total surgery time.

From the navigation display, the surgeons can intuitively identify the removed and residual tumour areas presented as 3D coloured models. This information can aid surgeons in complete removing tumour remnants. By producing a specific sound, our proposed system can also inform surgeons about whether they are working within the tumour area without disturbing the adjacent normal tissues; thus, surgeons can concentrate on the resection procedure without shifting their focus from the treatment area.

Materials and methods

In the present study, we applied our method to the data of five patients. In the Tokyo Women's Medical University Hospital, these patients underwent MRI-guided surgery with the 0.3-Tesla intra-operative MR imager AIRIS II (HITACHI, Tokyo, Japan). Prior to the surgery, informed consent for the use of the surgical navigation system was obtained from all patients, and any personal information was considered completely confidential. The patient data is summarised in Table 1.

Three-dimensional MR images were obtained using the following parameters: TR 1,000 ms; TE 140 ms; NEX 1; matrix 256 × 256; and scan order, axial IS. The patients had to be moved into the MR scanner during scanning, and moved out for the treatment. During surgery, the normal number of scans is fewer than three or four. Therefore, most of the tumour should be removed before the second or third scan.

Figure 1 depicts the overall process incorporating the proposed method.

Intra-operative segmentation of brain tumours

Intra-operative segmentation and 3D visualization of brain tumours assist surgeons in intuitively identifying the tumour position and margins. They also facilitate the quantitative measurement of the tumour size and volume during surgery. We used the fuzzy connectedness (FC) method to perform intra-operative segmentation of brain tumours. The FC method was first proposed for application in medical image segmentation, followed by reports on tumour segmentation using MRI [11–12]. Starting from a selected seed point in the tissue of interest (i.e. tumour), the method calculates the affinity of the neighbouring voxels based on two voxel criteria: their spatial closeness and the similarity of their image intensity. The algorithm automatically computes a fuzzy scene (a map of fuzzy connectivity) from the grey-scale images.

The FC method employed in this study requires two parameters: a seed point and a threshold for the fuzzy scene. The operator sets the seed point in the region of the tumour by clicking on one pixel displayed on the monitor. The operator also limits the region of analysis by enclosing the entire tumour in a rectangle and inputting the numbers of the first and last slices. This procedure reduces the processing time. A threshold is then set in the precomputed fuzzy scene. The robustness of the FC method can overcome the noise problems that are inherent to MR images. Since the ROI can be determined using a graphical user interface (GUI), the required processing time is less than 10 s with a standard Linux PC (CPU: Pentium 4, 2.53 GHz; RAM: 1024 MB); this speed is acceptable for intra-operative use.

Table 1 Patient data

Case	Age	Sex	Histological diagnosis	WHO grade	Location of the lesion
A	43	F	Anaplastic oligoastrocytoma	3	rt frontal lobe
B	39	F	Astrocytoma	2	lt insula
C	44	F	Anaplastic astrocytoma	3	rt insula-frontal lobe
D	30	F	Astrocytoma	2	lt frontal
E	52	F	Glioblastoma	4	rt parietal lobe

F female, *rt* right, *lt* left

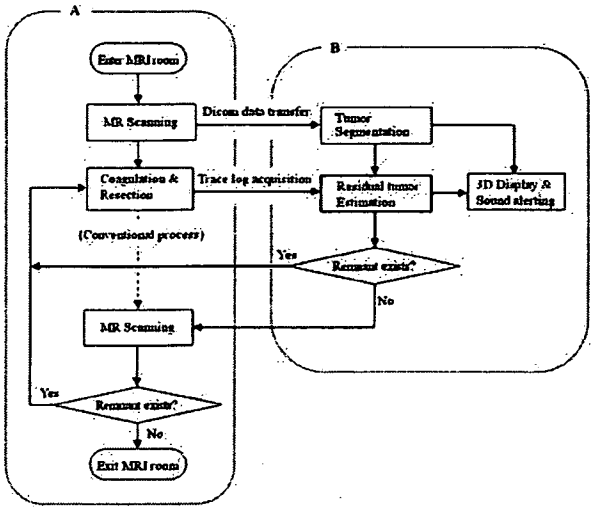

Fig. 1 *A* represents a conventional process; *B* represents the proposed process incorporated

To evaluate the performance of the FC segmentation, manual segmentation was performed by an expert neurosurgeon, and manual segmentation results were assumed to the standard. The neurosurgeon outlined the tumour boundaries on the images, and these were used for the comparison with the automatic segmentation. From the manual and automatic segmentation results, we calculated the percent match (PM) and dice similarity coefficient (DSC), both of which are equal to 1.0 when the results are perfectly matched [13].

Calculation and display of tumour remnants

The trace log can be obtained from the optical sensor Polaris (NDI, ON, Canada) that recognizes the position of the surgical device, to which optical markers are attached. Surgical procedures for brain tumour resection usually involve coagulation followed by cutting; therefore, the area that is coagulated using electrocautery can be regarded as the removed area. The trace recording in our system was updated at 1.5 Hz. The current method is applicable only when electrocautery is used for the resection process. For cases that do not require electrocautery, optical markers need to be attached to the different forceps that surgeons use, to collect the necessary trace data.

To estimate the removed area from the limited record of the trace log accurately, several additional processes were attempted as follows:

Setting of coagulation efficiency Since the trace of the log data consisted of a number of points with coordinates corresponding to the electrocautery position, the coagulated volume can be calculated from these points. The effects of coagulation on the tissues differs depending on the type and specifications of electrocautery. A parameter was designed for the setting of coagulation efficiency, and an appropriate value is chosen for each case.

Exclusion of invalid trace log Irrelevant data from the trace of log points should be eliminated. The trace log that is obtained while the surgeon rapidly moves the electrocautery device from one point to another should be excluded because the coagulation that occurs during this motion is insufficient or absent. This process involves checking the movement speed of the electrocautery device. This speed can be straightforwardly measured from the recorded positions in the trace log data. Finally, we select points that are located within the tumour and eliminate points that lie outside the tumour.

Inclusion of surrounded area To calculate the removed volume from the valid trace log, we constructed a volume by connecting each voxel that is regarded as being coagulated. However, this process yields an incomplete volume that does not include the interior of the tumour because surgeons tend to remove the brain tumour by accessing the tumour boundary without complete coagulation of the interior of the tumour, i.e., the interior of the tumour is actually removed without any trace log being recorded. Therefore, we added another process to include the interior of the tumour in the removed area. First, the centroid of the tumour is calculated from the segmentation results as described previously; then, each voxel adjacent to the line that connects the centroid to each valid log point is regarded as coagulated. By this process, we included the interior of the tumour where no trace log was recorded (Fig. 2).

Once the removed area is calculated, the residual tumour tissues are simply estimated by subtracting the removed area from the tumour segmentation results.

Finally, the removed and residual tumour areas are displayed in 3D and made available to the surgeons (Fig. 3). The open-source navigation software 3D Slicer (Brigham & Women's Hospital, Boston, USA) was employed to verify the clinical feasibility of the proposed method.

To validate the process of estimation and display of tumour remnants, we performed four retrospective studies and one clinical application.

Guidance for proper access to residual tumour tissues

By segmenting the tumour and estimating the remnant tumour area, surgeons can intuitively decide whether

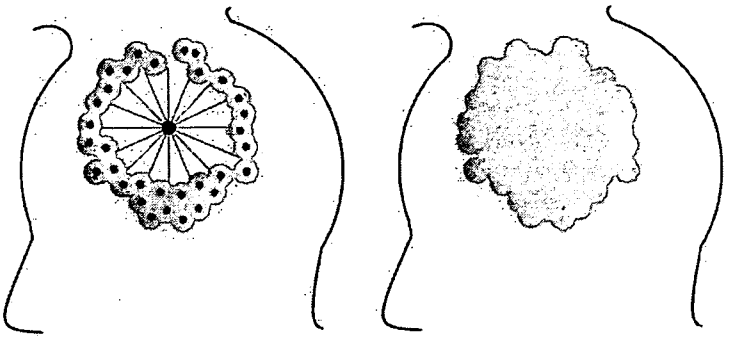

Fig. 2 The interior of the tumour where no trace log was recorded is included in the removed area. The *red points* represent the valid log points, the *pink points* represent the coagulation area, and the *green area* represents the removed area that was calculated from the trace log

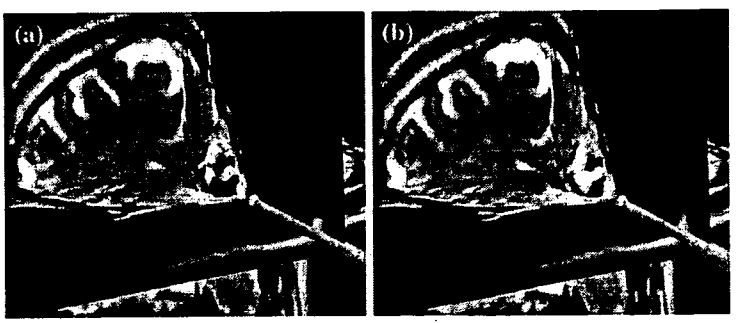

Fig. 3 Three-dimensional display of tumour resection. **a** The tumour in the early stage of the operation. The *blue area* represents the residual tumour tissue, and the *pink area* represents the coagulated and removed tissue. **b** The tumour in the late stage of the operation. Note that the residual tumour area is reduced in (**b**)

additional treatment is necessary, as shown in Fig. 3. However, when surgeons follow the navigation display, they cannot directly observe the tumour in the patient, and vice versa. This problem could disrupt the surgeons' concentration during surgery.

We developed a system that produces an alarm when the electrocautery device is located within the tumour. Thus, the surgeons could continue operating without shifting their focus from the patient. They can easily know whether they are working within or outside the tumour based on the alarm.

Since the resection time was short in the total surgical time, the surgeons set the system such that it sounded an alarm when the electrocautery device was inside the tumour rather than outside it.

Results

From the segmentation results, the average PM and DSC were 0.82 and 0.83, respectively. Tumour volume was also automatically calculated based on these results. The surgeon could track the size of the brain tumour and estimate the extra operation time on the basis of the tumour size. Figure 4 shows one of the segmentation results.

Figure 5 shows the effects of two additional processes that were proposed in this study for the accurate estimation of tumour remnants. The result presented in Fig. 5 was obtained from the data of clinical case E in which the trace log was collected carefully. Although the excluded invalid log data appeared to underestimate the removed area, it was considered to reflect the actually removed area but not the area that was merely in contact with the electrocautery device. For data from five patients, assuming that the resection rate by no additional process was 1.0, the resection rate by two additional processes was 1.16 ± 0.18. These processes were found to improve the accuracy of the estimation by the surgeons.

Figure 6 presents the changes in the rate at which the tumour tissue remained between the first and second scans during surgery. We observed the residual tumour tissues assumed to exist when the surgeons ended a resection following the first scan.

The sound alert system was also applied in over 20 clinical cases; in a qualitative evaluation, surgeons concluded that the system was very useful during the removal of tumours.

Discussion

This study showed that brain tumour segmentation and the intra-operative display of residual tumour tissues could assist the surgeon in accomplishing accurate tumour resection. In addition, the sound alert system proved to be useful in clinical application. We also

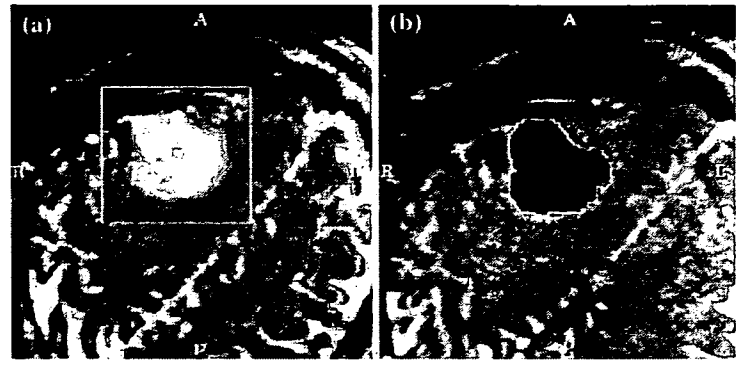

Fig. 4 Intra-operative brain tumour segmentation. **a** Initial setting for ROI. **b** Segmentation result; the *red area* represents the automatically segmented tumour, and the *line* represents the tumour boundary that was manually outlined by the surgeon

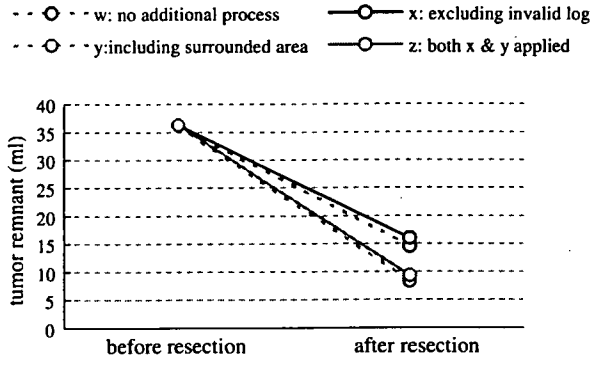

Fig. 5 Changes in tumour volume before the second scan. The excluding invalid trace log and the including the surrounded area by the valid trace log were applied for a more accurate estimation of the residual tumour tissues

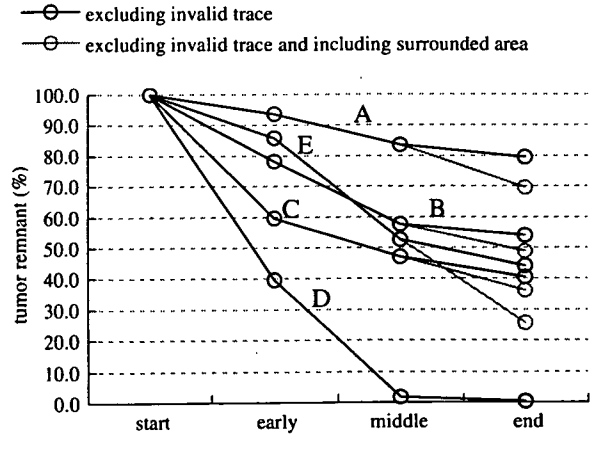

Fig. 6 Changes in the tumour tissue remaining during surgery in the five patients. After the surgeons conducted a resection following the first scan, the residual tumour tissue was estimated and displayed by analysing the trace log of electrocautery

proposed a useful process to estimate the tumour remnants accurately by excluding the invalid points in the trace log and including the surrounded area by the valid points. Although the final estimation still indicated considerable tumour remnant, for example over 25% in the case of E, this result can provide information on the direction in which surgeons should approach after subsequent scans.

However, we observed that the segmentation module did not produce accurate results when the tumour margins were obscured by the presence of edemas, ventricles, etc. If these errors are unacceptable to the surgeons, before estimating the tumour remnants, the errors can be partly edited using a manual procedure. To improve the accuracy of this method, future studies will be required to include knowledge-based parameters in the FC calculation.

As an offshoot of tumour segmentation, if the segmentation results are successfully obtained, the segmented region in the T2-weighted image could be overlaid on that in the T1-weighted image. In T2-weighted images, brain tumours show high intensities while other tissues are unclear; however, this is the opposite in the case of T1-weighted images. Therefore, overlaying the segmentation result in one image onto that of the other image can be advantageous.

Brain shift during surgery is another problem with regard to image-guided therapy [14–16]. Intra-operative MR scanning, however, provides the latest information following brain shift, which surgeons can observe at any time if required. Further, ultrasound could be an alternative modality for cases that require real-time observation of brain shift.

Figure 6 shows that, in several cases, surgeons could not remove approximately 50% of the tumour tissue before the second scan. This might represent an erroneous estimation even though following coagulations were assumed to be done with additional MR scanning. This is because the number of logs obtained from the optical sensor was too few for the system to estimate the removed and residual tumour tissues. Discontinuities in the trace log were due to the occurrence of obstacles in the visual path of the optical sensor, which

Table 2 Coverage of trace logs in the five patients

	A	B	C	D	E
Tumour (ml)	38.88	33.57	36.00	11.74	36.29
No. of points	3109	4271	6844	7456	15819
Coverage	79.97	127.22	184.99	634.93	435.91

Data were collected from four retrospective studies (A–D) and one clinical application (E)

is termed a line-of-sight problem. For an accurate estimation, we must obtain a sufficient number of trace logs.

Table 2 presents the coverage rate, which was calculated by dividing the tumour volume by the number of points from the trace log data as defined by,

$$\text{Coverage} = \frac{\text{tumour volume}}{\text{number of trace points}} \quad (1)$$

The data used for the retrospective studies had a small number of recorded points because the trace log data were not carefully collected before the proposed system was introduced. Therefore, the tumour remnant estimation was incomplete. In the clinical case, however, the data were carefully collected, and this case showed better estimation results.

To estimate the residual tumour tissues accurately, we considered a coverage of over 400 as necessary, based on the experiments. If the coverage is less than 400, the additional collection of trace data would be required. Therefore, during the surgery, sufficient trace log data should be carefully collected taking into consideration the visual path of the optical sensor. To overcome the line-of-sight problem, a magnetic position sensor can be used as an alternative tool, provided no magnetic disturbance occurs in the MRI room.

In this study, the percentages of tumor resection were defined by tumor identification based on MR images. Even if 100% resection is accomplished, glioma cells infiltrated within normal brain could still exist. However, 98% or more resection has been reported with significant survival advantage [17].

Conclusion

This study proposed a method for the intra-operative 3D display of the status of brain tumour resection to achieve accurate tumour removal. The intra-operative segmentation process reveals information on the tumour position and volume. Based on the tumour segmentation results, the removed and residual tumour areas are estimated using the trace log data of electrocautery. Therefore, surgeons can accurately approach the residual tumour tissues before or without additional MR scanning.

The production of an alarm when the tumour area is accessed was also useful. The results of four retrospective and a clinical pilot studies indicated the clinical feasibility of this method.

Acknowledgments The segmentation module was mainly developed by Mr. Takashi Inomata who graduated from the Graduate School of Information Science and Technology, University of Tokyo in 2005. We greatly appreciate his contribution.

References

1. Schulz T, Puccini S, Schneider J-P, Kahn T (2004) Interventional and intraoperative MR: review and update of techniques and clinical experience. Eur Radiol 14:2212–2227
2. Vannier MW, Haller JW (1999) Navigation in diagnosis and therapy. Eur J Radiol 31:132–140
3. Roberson PL, Mclaughlin PW, Narayana V, Troyer S, Hixson GV, Kessler ML (2005) Use and uncertainties of mutual information for computed tomography/magnetic resonance (CT/MR) registration post permanent implant of the prostate. Med Phys 32(2):473–482
4. Muragaki Y, Amano K, Iseki H, Kawamata T, Maruyama T, Takakura K, Hori T (2001) Initial experience of intraoperative MR imaging and "real-time" navigation. Societe Francaise De Neurochirurgie 15
5. Muragaki Y, Iseki H, Hori T (2001) The cerebral preservation neurosurgery using the navigator and open MRI. Symposium—brain mapping for surgical strategy. International Society for Brain Electromagnetic Topography 12th World Congress 28
6. Hiroshi I (2000) Image guided brain surgery. In: The 3rd Asian conference of neurological surgeons L17-2
7. Bao P, Warmath J, Galloway R Jr, Herline A (2005 Ultrasound-to-computer-tomography registration for image-guided laparoscopic liver surgery. Surg Endosc 19:424–429
8. Pagoulatos N, Edwards WS, Haynor DR, Kim Y (1999) Interactive 3D registration of ultrasound and magnetic resonance images based on a magnetic position sensor. IEEE Trans Inf Technol biomed 3(4):278–288
9. Tronnier VM, Bonsanto MM, Staubert A, Knauth M, Kunze S, Wirtz CR (2001) Comparison of intraoperative MR imaging and 3D-navigated ultrasonography in the detection and resection control of lesions. Neurosurg Focus 10(2):1–4
10. Slomka PJ, Mandel J, Downey D, Fenster A (2001) Evaluation of voxel-based registration of 3D power Doppler ultrasound and 3D magnetic resonance angiographic images of carotid arteries. Ultrasound Med Biol 27(7):945–955
11. Udupa JK, Samarasekera S (1999) Fuzzy connectedness and object definition: theory, algorithms, and applications in image segmentation. Graph Models Img Proc 9:85–90
12. Moonis G, Liu J, Udupa JK, Hackney DB (2002) Estimation of tumor volume with fuzzy-connectedness segmentation of MR images. AJNR Am J Neuroradiol 23:356–363
13. Hata N, Muragaki Y, Inomata T, Maruyama T, Iseki H, Hori T, Dohi T (2005) Intraoperative tumor segmentation and volume measurement in MRI-guided glioma surgery for tumor resection rate control. Acad Radiol 12(1):116–22

14. Hejazi N (2005) Frameless image-guided neuronavigation in orbital surgery: practical applications. Neurosurg Rev 23:1–5
15. Reinges MH, Nguyen HH, Krings T, Hutter BO, Rohde V, Gilsbach JM (2004) Course of brain shift during microsurgical resection of supratentorial cerebral lesions: limits of conventional neuronavigation. Acta Neurochir (Wien) 146:369–377
16. Roberts DW, Hartov A, Kennedy FE, Miga M, Paulsen KD (1998) Intraoperative brain shift and deformation: a quantitative analysis of cortical displacement in 28 cases. Neurosurgery 43(4):749–758
17. Lacroix M, Fourney DR, Gokaslan ZL, Shi W, DeMonte F, Lang FF, McCutcheon IE, Hassenbusch SJ, Holland E, Hess K, Michael C, Miller D, Sawaya R (2001) A multivariate analysis of 416 patients with glioblastoma multiforme: prognosis, extent of resection, and survival. J Neurosurg 95(2):190–8

ORIGINAL ARTICLE

Intraoperative diffusion-weighted imaging for visualization of the pyramidal tracts.

Part I: pre-clinical validation of the scanning protocol.

AUTHORS

N. Ozawa[1,4], Y. Muragaki[1,2], R. Nakamura[1,3], H. Iseki[1,2,3]

AFFILIATIONS

[1]Faculty of Advanced Techno-Surgery, Institute of Advanced Biomedical Engineering and Science;

[2]Department of Neurosurgery, Neurological Institute;

[3]International Research and Educational Institute for Integrated Medical Sciences (IREIIMS),

Tokyo Women`s Medical University, Tokyo, and

[4]MRI System Division, Hitachi Medical Corporation, Chiba,

Japan

CORRESPONDING AND REPRINT AUTHOR

prof. Hiroshi Iseki, M.D., Ph.D.

Faculty of Advanced Techno-Surgery, Institute of Advanced Biomedical Engineering and Science, Graduate School of Medicine, Tokyo Women`s Medical University, 8-1 Kawada-cho, Shinjuku-ku, Tokyo 162-8666, Japan

Phone: +81-3-3353-8111 (ext.39989), Fax: +81-3-5361-7796, E-mail: hiseki@abmes.twmu.ac.jp

SUMMARY

Integration of the intraoperative diffusion-weighted imaging (iDWI) into neuronavigation can be potentially useful for identification of the pyramidal tract during surgery for parenchymal brain lesions. Technique of iDWI using intraoperative MR scanner of low magnetic field strength (0.3 Tesla), was developed. For image acquisition a specially designed solenoid radiofrequency receiver coil integrated with modified Sugita head holder (headholder-coil) was used. While the sensitivity characteristics of the headholder-coil were found to be 29% lower compared to diagnostic quadrature head coil, these were sufficient enough to obtain iDWI images of good quality. The relationship between the angle of the motion probe gradient (MPG) pulse to the vertical axis and pyramidal tract contrasting was examined in 4 healthy men with a mean age of 30±5.7 years. The contrast ratio reached maximum when MPG pulse was applied exactly in the anteroposterior direction. The difference of the contrast ratio between right and left side was not statistically significant. Pyramidal tract visualization had becoming worse and contrast ratio was reduced when MPG pulse had been applied at different angles to the vertical axis; the reduction rate varied from 20.1% to 27.9% for each 15 degree of rotation irrespective of its side. In conclusion, developed scanning protocol for iDWI using originally designed headholder-coil allowed effective visualization of the pyramidal tracts using intraoperative MR scanner of low magnetic field strength.

KEY WORDS

intraoperative MRI

diffusion-weighted imaging

intraoperative neuronavigation

pyramidal tract

TEXT

Introduction

Introduction of the intraoperative magnetic resonance imaging (iMRI) revolutionized management of parenchymal brain tumors and created principally new options for their radical and safe resection [1-4]. Currently not only structural but functional and metabolic iMRI techniques found an acceptance during surgery of gliomas. Particularly, diffusion tensor imaging (DTI) can be useful for intraoperative identification of the motor white matter tracts and their differentiation from the sensory ones [5]. However, operator-depending DTI-based fiber tracking is susceptible for underestimation of the exact size of the pyramidal tract and can erroneously define its position [6,7]. On the contrary, identification of the white matter tracts with diffusion-weighted imaging (DWI) does not require user participation. Integration of the DWI into intraoperative neuronavigation during surgery for parenchymal brain lesions can potentially provide nearly real-time information about spatial interrelationships between pyramidal tract, the lesion, and position of the surgical instrument, including electrical stimulator for subcortical functional mapping, which can be preventive for inadvertent tract injury and useful in avoidance of postoperative deterioration of the motor function. Technique of intraoperative DWI (iDWI) using intraoperative MR scanner of low magnetic field strength (0.3 Tesla), has been developed recently in Tokyo Women`s Medical University [8,9]. Validation of the scanning protocol constituted the objective of the pre-clinical part of the present study.

Methods and Materials

iDWI was developed using intraoperative MR scanner (AIRIS II, Hitachi Medical, Tokyo, Japan), which is available in the "intelligent operating theater" of the Tokyo Women`s Medical University, and equipped with disc-shaped permanent magnet with a magnetic field strength of 0.3 Tesla (gradient up to 15 mT/m). For acquisition of iDWI a specially developed solenoid radiofrequency receiver coil with a cupper wire built in the modified Sugita head holder (Headholder-coil; Mizuho Ltd., Tokyo, Japan) was used. The detailed characteristics of the device are provided elsewhere [10]. It is made from glass-fiber reinforced plastic in order to prevent susceptibility artifacts on iMRI. Titanium fixation pins provides both stable position of the patient head during surgery and prevention of the image artifacts. Positioning of the coil in the vicinity to the visualized region results

in optimal image quality and high sensitivity.

Requirements for iDWI were formulated as following: (1) possibility to visualize the white matter tracts, particularly pyramidal tract, during surgery for parenchymal brain lesions; (2) optimal coil sensitivity providing sufficient image resolution for unequivocal interpretation of the obtained data by neurosurgeon; (3) reasonable time required for image acquisition, which can fulfill the needs of the real surgical situation; (4) avoidance of image artifacts, which can lead to mislocalization errors during neuronavigation; (5) positional accuracy within 5 mm during use for intraoperative neuronavigation. To fulfill these requirements the pre-clinical study was separated into two main parts: testing of the sensitivity characteristics of the headholder-coil for their correspondence to requirements of iDWI, and validation of the scanning protocol on healthy volunteers to confirm the accuracy of iDWI for visualization of the pyramidal tract. The study was approved by responsible authorities of the Tokyo Women`s Medical University and informed consent was obtained from each volunteer.

Testing of sensitivity characteristics of the headholder-coil

To confirm that headholder-coil can be used for iDWI its sensitivity characteristics were compared with diagnostic quadrature (QD) head coil. Axial multi-slice spin echo images of a cylindrical nickel chloride phantom (18 mmol/L, 160 mm in diameter) positioned at the center of the headholder-coil were obtained using TR 800 msec and TE 20 msec. For each slice the signal-to-noise ratio within region-of-interest (120 mm in diameter) was measured for sensitivity characteristics in the direction perpendicular to the coil (craniocaudal direction – Z-axis). Signal profiles of the acquired images were measured in the directions parallel to the coil (horizontal (mediolateral) direction – X-axis and vertical (anteroposterior) direction – Y-axis). The same measurements were done with a diagnostic QD head coil.

Validation of the scanning protocol

For acquisition of DWI motion probing gradient (MPG) pulse should be applied in the anteroposterior direction, which in cases of intraoperative imaging is turned away from the vertical axis due to rotation of the patient head and its fixation in the head holder. The relationship between the angle of MPG pulse and pyramidal tract

contrasting was examined in 4 healthy men with a mean age of 30±5.7 years (range: 24 – 37 years). A volunteer was positioned supine on the operating table without any sedation and his head was immobilized with a plastic band. The operating table was moved into gantry gap of the intraoperative MR scanner and coronal four shots pulse-triggered diffusion-weighted spin-echo echo-planar imaging with fat suppression were performed after shimming using diagnostic QD head coil. The scanning parameters were as follows: TE 111msec; FOV 250 mm; scan matrix size 100 × 92; reconstruction matrix size 256 × 256; b-value 700 sec/mm^2; thickness 8 mm; 18 slices to cover the pyramidal tract; 8 excitations. For providing the optimal resolution a slice interval was set at 3 mm. Data acquisition was divided into three parts, which were interleaved for prevention of the interference between slices (1st acquisition: 1, 4, 7, etc; 2nd acquisition: 2, 5, 8, etc; 3rd acquisition: 3, 6, 9, etc.). For suppression of the motion artifacts, time delay from the systole was set on more than 300 msec [11]. Craniocaudal phase encoding was applied in order to prevent mediolateral image distortion corresponded to the usual direction of the surgical manipulations. The scanning time varied from 5 to 10 min.

For simulation of the patient head rotation during surgery sequential DWI were performed with applying of the MPG pulses at different angles (θ) to the vertical axis (0, ± 15, ± 30, ± 45, ± 90 degrees, where positive values correspond to the rotation to the left, and negative – to the right). For evaluation of the visualization quality the contrast ratios between white matter tracts including the pyramidal tract (signal I_p) and thalamic area including upper brainstem (signal I_t) were calculated as $(I_p-I_t)/I_t \times 100$ (%). The angle, which provided the optimum contrasting of the pyramidal tract was identified and tract visualization on both sides was compared.

Statistics

Two-tailed t-test was used for statistical analysis. The level of significance level was determined at $P < 0.05$.

Results

Testing of sensitivity characteristics of the headholder-coil

The sensitivity of the headholder-coil at its center was in average 29% lower compared to the diagnostic QD head coil (Fig. 1). The sensitivity characteristics in X-axis and Z-axis were symmetrical in relation to the coil center,

whereas the sensitivity in Y-axis was asymmetrical and its reduction was marked in the upper side.

Validation of the scanning protocol

The contrast ratio reached maximum when MPG pulse was applied exactly in the anteroposterior direction ($\theta = 0$ degree), and constituted in average 40.7 ± 10.8 % with a range from 59.4% to 30.7% (Fig.2). It permitted optimal differentiating of the pyramidal tracts from surrounding cerebral tissue. The difference of the contrast ratio between right and left side was not statistically significant. Pyramidal tract visualization had becoming worse and contrast ratio was reduced when MPG pulse had been applied at different angles to the vertical axis; the reduction rate varied from 20.1% to 27.9% for each 15 degree of θ irrespective to its polarity.

Discussion

Up to date there are limited number of reports about intraoperative acquisition of DWI and DTI for visualization of the white matter tracts [12,13]. This can be particularly caused by known technical difficulties of these techniques, which resulted from association of the required echo-planar imaging (EPI) with susceptibility artifacts, image distortion in single-shot imaging, and motion artifacts in multi-shot imaging [14-17]. Moreover, DTI-based tractography may underestimate the exact size and location of the white matter tracts [6]. Kinoshita et al. [7] reported mismatch between data of the subcortical functional brain mapping with electrical stimulation and information obtained with DTI-based neuronavigation, used for intraoperative identification of the motor tracts location. In the same time, integration of the DWI and DTI into intraoperative neuronavigation during surgery for parenchymal brain lesions can be done only if image distortion will be avoided and underestimation of the tract size and position will be minimized.

It is known, that image distortion caused by susceptibility artifacts is less if MR scanners with low magnetic field strength are used. However, single-shot EPI performed in such a scanner suffers from image distortion due to poor magnetic field homogeneity of the permanent magnet and necessitates use of multi-shot EPI, which is less associated with image distortion. Originally developed headholder-coil provided sufficient sensitivity in its center, where the patient head and operative field is actually located, which resulted in optimal quality and accuracy of

iDWI. The expected lower sensitivity characteristics of the headholder-coil compared to the diagnostic QD head coil in all the direction is resulted from single solenoid nature of the former. About 33% decrease of the coil sensitivity 75 mm cranially from its center along Z-axis, which was found in the present study, is well corresponded to the data reported by Staubert et al. [18]. The asymmetric sensitivity profile in Y-axis seems attributable to the coil ellipsoidal shape, but did not result in reduction of quality of the intraoperative images.

DWI-based identification of the pyramidal tract does not require operator participation, and seems to be promising in precise identification of the tract size and position. Pre-clinical testing of the developed scanning protocol for iDWI permitted clear visualization of the pyramidal tracts in all cases. In concordance with previously published data [19] application of the MPG pulse along the anteroposterior direction was found to be optimal. Under such setting, the contrasting of the pyramidal tract, which is running craniocaudally, was enhanced due to suppression of the signal of the other white matter tracts, such as superior longitudinal fasciculus, which are running anteroposteriorly.

In conclusion, the results of the present pre-clinical study show, that developed scanning protocol for iDWI using original solenoid radiofrequency receiver coil integrated with modified Sugita head holder allowed effective visualization of the pyramidal tracts using intraoperative MR scanner of low magnetic field strength (0.3 Tesla). Image quality, resolution, and accuracy were proved to be sufficient enough for further clinical testing with integration into intraoperative neuronavigation system during surgery for parenchymal brain lesions.

Acknowledgements

The authors are thankful to Drs. Tomokatsu Hori, Mikhail Chernov, Kyojiro Nambu and Yuji Okawara (Tokyo Women`s Medical University) and Dr. Thomas Georg Gasser (University of Duisburg-Essen) for invaluable advices and help with preparation of the manuscript. This work was supported by the Program for Promoting the Establishment of Strategic Research Centers, Special Coordination Funds for Promoting Science and Technology, Ministry of Education, Culture, Sports, Science and Technology (Japan).

References

1. Black PM, Moriarty T, Alexander EIII, Stieg P, Woodard EJ, Gleason PL, Martin CH, Kikinis R, Schwartz RB, Jolesz FA. Development and implementation of intraoperative magnetic resonance imaging and its neurosurgical applications. Neurosurgery 1997; 41: 831 – 845
2. Sutherland GR, Kaibara T, Louw D, Hoult DI, Tomanek B, Saunders J. A mobile high-field magnetic resonance system for neurosurgery. J Neurosurg 1999; 91: 804 – 813
3. Nimsky C, Ganslandt O, Cerny S, Hastreiter P, Greiner G, Fahlbusch R. Quantification of, visualization of, and compensation for brain shift using intraoperative magnetic resonance imaging. Neurosurgery 2000; 47: 1070 – 1080
4. Muragaki Y, Iseki H, Maruyama T, Kawamata T, Yamane F, Nakamura R, Kubo O, Takakura K, Hori T. Usefulness of intraoperative magnetic resonance imaging for glioma surgery. Acta Neurochir Suppl 2006; 98: 67 – 75
5. Yamada K, Kizu O, Mori S, Ito H, Nakamura H, Yuen S, Kubota T, Tanaka O, Akada W, Sasajima H, Mineura K, Nishimura T. Brain fiber tracking with clinically feasible diffusion-tensor MR imaging: initial experience. Radiology 2003; 227: 295 – 301
6. Clark CA, Barrick TR, Murphy MM, Bell BA. White matter fiber tracking in patients with space-occupying lesions of the brain: a new technique for neurosurgical planning ? Neuroimage 2003; 20: 1601 – 1608
7. Kinoshita M, Yamada K, Hashimoto N, Kato A, Izumoto S, Baba T, Maruno M, Nishimura T, Yoshimine T. Fiber-tracking does not accurately estimate size of fiber bundle in pathological condition: initial neurosurgical experience using neuronavigation and subcortical white matter stimulation. Neuroimage 2005; 25: 424 – 429
8. Ozawa N, Muragaki Y, Shirakawa H, Suzukawa K, Nakamura R, Watanabe S, Iseki H, Takakura K. Development of navigation system employing intraoperative diffusion weighted imaging using open MRI. In: Lemke HU, Vannier MW, Inamura K, Farman AG, Doi K, Reiber JHC (eds). Computer assisted radiology and surgery: Proceedings of the 18th International Congress and Exhibition. Amsterdam: Elseiver, 2004: 697 – 702
9. Ozawa N, Muragaki Y, Shirakawa H, Suzukawa H, Nakamura R, Iseki H. Navigation system based on intraoperative diffusion weighted imaging using open MRI. In: Lemke HU, Inamura K, Doi K, Vannier MW,

Farman AG (eds). Computer assisted radiology and surgery: Proceedings of the 19th International Congress and Exhibition. Amsterdam: Elseiver, 2005: 810 – 814

10. Taniguchi H, Muragaki Y, Iseki H, Nakamura R, Taira T. New radiofrequency coil integrated with a stereotactic frame for intraoperative MRI-controlled stereotactically guided brain surgery. Stereotact Func Neurosurg 2006; 84: 136 – 141

11. Jiang H, Golay X, van Zijl PC, Mori S. Origin and minimization of residual motion-related artifacts in navigator-corrected segmented diffusion-weighted EPI of the human brain. Magn Reson Med 2002; 47: 818 – 822

12. Mamata Y, Mamata H, Nabavi A, Kacher DF, Pergolizzi RS Jr, Schwartz RB, Kikinis R, Jolesz FA, Maier SE. Intraoperative diffusion imaging on a 0.5 Tesla interventional scanner. J Magn Reson Imaging 2001; 13: 115 – 119

13. Nimsky C, Ganslandt O, Hastreiter P, Wang R, Benner T, Sorensen AG, Fahlbusch R. Preoperative and intraoperative diffusion tensor imaging-based fiber tracking in glioma surgery. Neurosurgery 2005; 56: 130 – 138

14. Mansfield P. Multi-planar image formation using NMR spin echoes. J Phys Chem 1977; 10: 155 – 158

15. Anderson AW, Gore JC. Analysis and correction of motion artifacts in diffusion weighted imaging. Magn Reson Med 1994; 32: 379 – 387

16. Rohde GK, Barnett AS, Basser PJ, Marenco S, Pierpaoli C. Comprehensive approach for correction of motion and distortion in diffusion-weighted MRI. Magn Reson Med 2004; 51: 103 – 114

17. Neufeld A, Assaf Y, Graif M, Hendler T, Navon G. Susceptibility-matched envelope for the correction of EPI artifacts. Magn Reson Imaging 2005; 23: 947 – 951

18. Staubert A, Pastyr O, Echner G, Oppelt A, Vetter T, Schlegel W, Bonsanto MM, Tronnier VM, Kunze S, Wirtz CR. An integrated head-holder/coil for intraoperative MRI in open neurosurgery. J Magn Reson Imaging 2000; 11: 564 – 567

19. Krings T, Reinges MHT, Thiex R, Gilsbach JM, Thron A. Functional and diffusion-weighted magnetic resonance images of space-occupying lesions affecting the motor system: imaging the motor cortex and pyramidal tracts. J Neurosurg 2001; 95: 816 – 824

LEGENDS FOR FIGURES

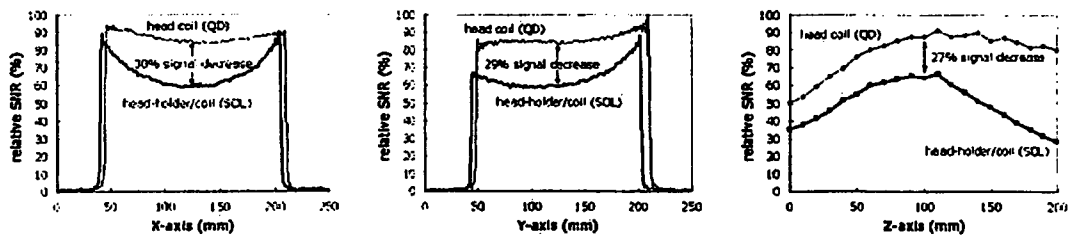

Figure 1

Comparison of sensitivity characteristics of the solenoid (SOL) radiofrequency receiver coil integrated with modified Sugita head holder for intraoperative MRI (headholder-coil) and diagnostic quadrature (QD) head coil. X-axis: horizontal direction, left side was considered positive; Y-axis: vertical direction, downside was considered positive; Z-axis: craniocaudal direction, perpendicular to the coil, cranial side was considered positive. Although the headholder-coil sensitivity was lower than that of QD head coil, it was sufficient to obtain DWI images of good quality and accuracy. SNR: signal-to-noise ratio.

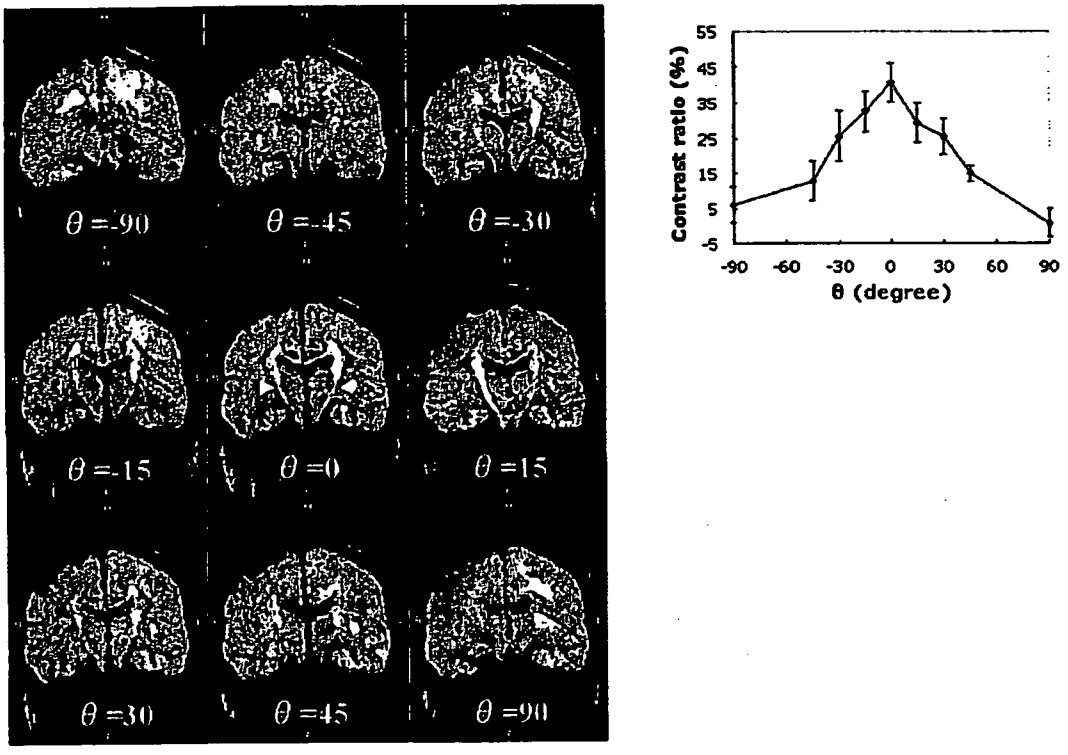

Figure 2

Influence of motion probing gradient (MPG) pulse direction on the visualization of pyramidal tracts. Left: coronal DWI obtained in volunteers with quadrature (QD) head coil using different directions of the MPG pulse (θ – the angle to the vertical axis (anteroposterior direction); positive values correspond to rotation to the left, whereas negative – to the right). Right: interrelationships between MPG pulse angle (θ) and contrast ratio between white matter tracts including the pyramidal tract and thalamus region including the upper brainstem. Note that the contrasting of the pyramidal tract was optimum at θ = 0 degree (*arrowheads*).

ORIGINAL ARTICLE

Intraoperative diffusion-weighted imaging for visualization of the pyramidal tracts.

Part II: clinical study of usefulness and efficacy

AUTHORS

N. Ozawa[1,4], Y. Muragaki[1,2], R. Nakamura[1,3], H. Iseki[1,2,3]

AFFILIATIONS

[1]Faculty of Advanced Techno-Surgery, Institute of Advanced Biomedical Engineering and Science;

[2]Department of Neurosurgery, Neurological Institute;

[3]International Research and Educational Institute for Integrated Medical Sciences (IREIIMS),

Tokyo Women`s Medical University, Tokyo, and

[4]MRI System Division, Hitachi Medical Corporation, Chiba,

Japan

CORRESPONDING AND REPRINT AUTHOR

prof. Hiroshi Iseki, M.D., Ph.D.

Faculty of Advanced Techno-Surgery, Institute of Advanced Biomedical Engineering and Science, Graduate School of Medicine, Tokyo Women`s Medical University, 8-1 Kawada-cho, Shinjuku-ku, Tokyo 162-8666, Japan

Phone: +81-3-3353-8111 (ext.39989), Fax: +81-3-5361-7796, E-mail: hiseki@abmes.twmu.ac.jp

SUMMARY

Precise identification and preservation of the pyramidal tract during surgery for parenchymal brain tumors is of crucial importance for avoidance of postoperative deterioration of the motor function. Technique of intraoperative diffusion-weighted imaging (iDWI) using intraoperative MR scanner of low magnetic field strength (0.3 Tesla) has been developed. Its clinical usefulness and efficacy were evaluated in 10 surgically treated patients with gliomas (5 men and 5 women; mean age of 41.2 ± 13.9 years). iDWI permitted visualization of the pyramidal tract on the non-affected side in all 10 cases, and on the affected side in 8 cases. Motion artifacts were observed in four patients, but were not an obstacle for identification of the pyramidal tract. Good correspondence of the anatomical landmarks localization on iDWI and T_1-weighted imaging was found. All participating neurosurgeons agreed, that in the majority of cases iDWI was very useful for localization of the pyramidal tract and for clarification of its spatial relationships with the tumor. In conclusion, image quality and accuracy of the iDWI obtained with MR scanner of low magnetic field strength (0.3 Tesla) is sufficient for possible incorporation into intraoperative neuronavigation system. Using of iDWI in addition to structural iMRI and subcortical functional mapping with electrical stimulation can potentially result in reduction of the postoperative morbidity after aggressive surgical removal of lesions located in the vicinity to the motor white matter tracts.

KEY WORDS

intraoperative MRI

diffusion-weighted imaging

intraoperative neuronavigation

pyramidal tract